5180 *Inorg. Chem.* **2010**, *49*, 5180–5189
DOI: 10.1021/ic1003116

Inorganic Chemistry
Article

Effect of Sulfur-Based Substituents on the Electronic Properties of Re(I) dppz Complexes

Michael G. Fraser, Allan G. Blackman, Garth I. S. Irwin, Campbell P. Easton, and Keith C. Gordon*

MacDiarmid Institute for Advanced Materials and Nanotechnology, Department of Chemistry, University of Otago, Dunedin 9001, New Zealand

Received February 14, 2010

A series of sulfur-substituted dppz-based ligands and their $Re(I)(CO)_3Cl$ complexes are reported. The sulfur-substituted ligands and complexes show interesting electronic properties atypical of dppz-type systems. Substitution of dppz with thiocyanate (SCN) groups results in behavior typical of an electron withdrawing group. However, substitution of dppz with the electron donating trithiocarbonate (S_2CS) or deca-alkylthioether (Sdec) groups confer intraligand charge-transfer (ICT) from the S adduct to the phenazine lowest unoccupied molecular orbital (LUMO). Upon complexation of the substituted dppz ligand to $Re(CO)_3Cl$ this ICT red-shifts and increases in intensity. Analysis of these observations using density functional theory (DFT) calculations and resonance Raman spectroscopy reveals that these transitions are a mixture of metal-to-ligand charge-transfer (MLCT) and S → phenazine ICT in nature. The synthesized compounds are also characterized using ^{1}H NMR spectroscopy, IR spectroscopy, and electrochemistry. Single-crystal X-ray analysis was performed on $dppz(SCN)_2$ ($C_{20}H_{18}N_6S_2$ a = 8.780 Å, b = 9.792 Å, c = 10.400 Å, α = 95.95°, β = 112.13°, γ = 95.38°, triclinic, $P\bar{1}$, Z = 2, R1 = 0.0306, wR2 = 0.0829.

Introduction

Complexes incorporating dipyrido[3,2-*a*:2′,3′-*c*]phenazine (dppz) and its derivatives have been the subject of extensive investigation because they possess interesting photophysical properties.[1−5] One striking example of this is the observation that some dppz complexes exhibit a "light switch effect", being highly emissive in aqueous solution in the presence of DNA but non-emissive in normal aqueous solution.[6−10] Theoretical and photophysical studies suggest that the excited states of Re(I) complexes with dppz-type ligands contain closely lying ligand centered (LC) and metal-to-ligand charge-transfer (MLCT) states of differing orbital parentage. The orbital parentage of electronic transitions in dppz has been the subject of some early theoretical investigations which remain the current thinking on the electronic structure of the ligand.[2,11−15] In dppz the lowest lying unoccupied molecular orbitals (MOs) may have phenanthroline character, b_1(phen), in which the wave function amplitude is predominantly across the A, B, and C rings (Figure 1)

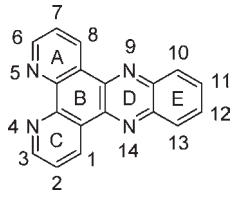

Figure 1. Dppz ligand structure with ring labels and numbering.

*To whom correspondence should be addressed. E-mail: kgordon@chemistry.otago.ac.nz.

(1) Amouyal, E.; Homsi, A.; Chambron, J. C.; Sauvage, J. P. *J. Chem. Soc., Dalton Trans.* **1990**, 1841–1845.
(2) Fees, J.; Kaim, W.; Moscherosch, M.; Matheis, W.; Klima, J.; Krejcik, M.; Zalis, S. *Inorg. Chem.* **1993**, *32*, 166–174.
(3) Stoeffler, H. D.; Thornton, N. B.; Temkin, S. L.; Schanze, K. S. *J. Am. Chem. Soc.* **1995**, *117*, 7119–7128.
(4) Coates, C. G.; Jacquet, L.; McGarvey, J. J.; Bell, S. E. J.; Al-Obaidi, A. H. R.; Kelly, J. M. *J. Am. Chem. Soc.* **1997**, *119*, 7130–7136.
(5) Elias, B.; Creely, C.; Doorley, G. W.; Feeney, M. M.; Moucheron, C.; Kirsch-DeMesmaeker, A.; Dyer, J.; Grills, D. C.; George, M. W.; Matousek, P.; Parker, A. W.; Towrie, M.; Kelly, J. M. *Chem.—Eur. J.* **2008**, *14*, 369–375.
(6) Barton, J. K. *Science* **1986**, *233*, 727–734.
(7) Broo, A.; Lincoln, P. *Inorg. Chem.* **1997**, *36*, 2544–2553.
(8) Coates, C. G.; Olofsson, J.; Coletti, M.; McGarvey, J. J.; Oenfelt, B.; Lincoln, P.; Norden, B.; Tuite, E.; Matousek, P.; Parker, A. W. *J. Phys. Chem. B* **2001**, *105*, 12653–12664.
(9) Olofsson, J.; Onfelt, B.; Lincoln, P.; Norden, B.; Matousek, P.; Parker, A. W.; Tuite, E. *J. Inorg. Biochem.* **2002**, *91*, 286–297.
(10) Westerlund, F.; Pierard, F.; Eng, M. P.; Norden, B.; Lincoln, P. *J. Phys. Chem. B* **2005**, *109*, 17327–17332.
(11) Klein, A.; Kaim, W.; Waldhoer, E.; Hausen, H.-D. *J. Chem. Soc., Perkin Trans. 2* **1995**, 2121–2126.
(12) Chambron, J. C.; Sauvage, J. P.; Amouyal, E.; Koffi, P. *New. J. Chem.* **1985**, *9*, 527–529.
(13) Atsumi, M.; Gonzalez, L.; Daniel, C. *J. Photochem. Photobiol., A* **2007**, *190*, 310–320.
(14) Dyer, J.; Blau, W. J.; Coates, C. G.; Creely, C. M.; Gavey, J. D.; George, M. W.; Grills, D. C.; Hudson, S.; Kelly, J. M.; Matousek, P.; McGarvey, J. J.; McMaster, J.; Parker, A. W.; Towrie, M.; Weinstein, J. A. *Photochem. Photobiol. Sci.* **2003**, *2*, 542–554.
(15) Kuimova, M. K.; Alsindi, W. Z.; Dyer, J.; Grills, D. C.; Jina, O. S.; Matousek, P.; Parker, A. W.; Portius, P.; Sun, X. Z.; Towrie, M.; Wilson, C.; Yang, J.; George, M. W. *Dalton Trans.* **2003**, 3996–4006.

 Published on Web 05/13/2010

or phenazine character, b_1(phz), in which the amplitude is on the B, D, and E rings.

In this sense they are segregated MOs. There is also a third low-lying delocalized a_2 MO. These states can be alternatively tuned in energy by chelation of the ligand to various metals, thus affecting the b_1(phen) MO, or by substitution at the E-ring, thereby altering the energy of the b_1(phz) MO.[16−22] The basis of the "light switch effect" is the energetics of these states. The metal-phz MLCT state is termed the dark state and is non-emissive. Olson et al.[23] suggested that this is the lowest excited state in protic solvents because the phz nitrogen atoms become protonated and this causes stabilization of the excited state. The luminescence is therefore quenched, and non-radiative decay is from the dark state. Brennaman et al.[24] showed that the M→phen MLCT state is entropically favored over the enthalpically favored M→phz "dark" state. This is because the dark state involves a more significant reorganization of solvent because of its greater charge separation. Substitution at both the 11 and 12, and 2 and 7, positions on dppz has been studied, and in both cases perturbation of the interplay of states in the ligand and its complexes was found.[25−31] Understanding the processes which occur in dppz complexes is vital to the development of rationally designed complexes for applications in photoelectrochemical cells[32] and therapeutic drugs.[33,34]

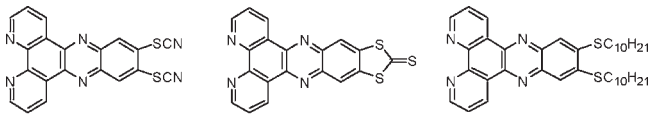

a) dppz(SCN)$_2$ b) dppzS_2CS c) dppz(Sdec)$_2$

Figure 2. Sulfur substituted dppz based ligands in this study.

Recently a tetrathiofulvalene substituted dppz ligand has been used to create a donor−acceptor ensemble in which the fulvalene unit acts to donate charge to the b_1(phz) orbital thus creating a new electronic transition to the dppz systems.[35,36] Also, dppz substituted with octadecanethioether groups has been prepared for incorporation in metallomesogen compounds.[37]

In this paper we report results of sulfur-containing dppz-type ligands in which the degree of charge donation to the phz ring system is altered. We have investigated three dppz-based ligands in which differing sulfur-bearing substituents are appended (Figure 2). We find that for the trithiocarbonate and thioether ligands there is strong intraligand charge-transfer (ICT) character in the electronic structure of both the ligands and their complexes; this effect is much smaller in the dppz(SCN)$_2$ ligand as SCN behaves as a normal electron-withdrawing phz substituent. In the Re(L)(CO)$_3$Cl complexes (L = dppzS_2CS, dppz(Sdec)$_2$) this ICT increases in intensity and a new band appears around 330 nm for both complexes. These features are analyzed using density functional theory (DFT) calculations and resonance Raman spectroscopy to reveal that the nature of these transitions is a mixture between MLCT and S → phenazine ICT.

Experimental Section

Materials. Commercially available reagents were used as received. Literature procedures were used to prepare 1,10-phenanthroline-5,6-dione,[38] 1,2 diamino-benzene-4,5-bis(thiocyanate),[39] and 5,6-diamino-1,3-benzodithiol-2-thione.[40] Dppz ligands were synthesized by the Schiff base condensation of 1,10-phenanthroline-5,6-dione with the appropriate diamino compound. 11,12-Bis-(decaalkylthioether)dipyridophenazine was synthesized by the method of Kestemont et al.[41] The rhenium complexes were synthesized as previously reported.[42]

Dipyrido[3,2-*a*:2′,3′-*c*]phenazine-11,12 bis(thiocyanate) (dppz-(SCN)$_2$) (1). Yield = 0.54 g, 63%. ^{1}H NMR (300 MHz CDCl$_3$) δ 9.61 (dd, 2H, J = 1.5 Hz, 8.1 Hz), 9.34 (dd, 2H, J = 1.8 Hz, 4.5 Hz), 8.87 (s, 2H), 7.87 (dd, 2H, J = 4.5, 8.1) ppm. Anal. Calcd for $C_{22}H_{14}N_6S_2$; C 60.30, H 2.41, N 20.49. Found: C 60.26, H 2.15, N 20.36. M/z (ESI POS): 419.01 {[dppz(SCN)$_2$] + Na^+}.

(16) Waterland, M. R.; Gordon, K. C. *J. Raman Spectrosc.* **2000**, *31*, 243–253.
(17) McGarvey, J. J.; Callaghan, P.; Coates, C. G.; Schoonover, J. R.; Kelly, J. M.; Jacquet, L.; Gordon, K. C. *J. Phys. Chem. B* **1998**, *102*, 5941–5942.
(18) Lundin, N. J.; Walsh, P. J.; Howell, S. L.; McGarvey, J. J.; Blackman, A. G.; Gordon, K. C. *Inorg. Chem.* **2005**, *44*, 3551–3560.
(19) Walsh, P. J.; Gordon, K. C.; Lundin, N. J.; Blackman, A. G. *J. Phys. Chem. A* **2005**, *109*, 5933–5942.
(20) Berger, S.; Fiedler, J.; Reinhardt, R.; Kaim, W. *Inorg. Chem.* **2004**, *43*, 1530–1538.
(21) Fees, J.; Ketterle, M.; Klein, A.; Fiedler, J.; Kaim, W. *J. Chem. Soc., Dalton Trans.* **1999**, 2595–2600.
(22) Matthewson, B. J.; Flood, A.; Polson, M. I. J.; Armstrong, C.; Phillips, D. L.; Gordon, K. C. *Bull. Chem. Soc. Jpn.* **2002**, *75*, 933–942.
(23) Olson, E. J. C.; Hu, D.; Hormann, A.; Jonkman, A. M.; Arkin, M. R.; Stemp, E. D. A.; Barton, J. K.; Barbara, P. F. *J. Am. Chem. Soc.* **1997**, *119*, 11458–11467.
(24) Brennaman, M. K.; Alstrum-Acevedo, J. H.; Fleming, C. N.; Jang, P.; Meyer, T. J.; Papanikolas, J. M. *J. Am. Chem. Soc.* **2002**, *124*, 15094–15098.
(25) Schwalbe, M.; Karnahl, M.; Tschierlei, S.; Uhlemann, U.; Schmitt, M.; Dietzek, B.; Popp, J.; Groake, R.; Vos, J. G.; Rau, S. *Dalton Trans* **2010**, *39*, 2768–2771.
(26) Kuhnt, C.; Karnahl, M.; Tschierlei, S.; Griebenow, K.; Schmitt, M.; Schafer, B.; Krieck, S.; Gorls, H.; Rau, S.; Dietzek, B.; Popp, J. *Phys. Chem. Chem. Phys.* **2010**, *12*, 1357–1368.
(27) Dyer, J.; Grills, D. C.; Matousek, P.; Parker, A. W.; Towrie, M.; Weinstein, J. A.; George, M. W. *Chem. Commun.* **2002**, 872–873.
(28) Kuimova, M. K.; Grills, D. C.; Matousek, P.; Parker, A. W.; Sun, X.-Z.; Towrie, M.; George, M. W. *Vib. Spectrosc.* **2004**, *35*, 219–223.
(29) Dyer, J.; Creely, C. M.; Penedo, J. C.; Grills, D. C.; Hudson, S.; Matousek, P.; Parker, A. W.; Towrie, M.; Kelly, J. M.; George, M. W. *Photochem. Photobiol. Sci.* **2007**, *6*, 741–748.
(30) Kuimova, M. K.; Sun, X. Z.; Matousek, P.; Grills, D. C.; Parker, A. W.; Towrie, M.; George, M. W. *Photochem. Photobiol. Sci.* **2007**, *6*, 1158–1163.
(31) Kuimova, M. K.; Alsindi, W. Z.; Blake, A. J.; Davies, E. S.; Lampus, D. J.; Matousek, P.; McMaster, J.; Parker, A. W.; Towrie, M.; Sun, X. Z.; Wilson, C.; George, M. W. *Inorg. Chem.* **2008**, *47*, 9857–9869.
(32) Kalyanasundaram, K.; Gratzel, M. *Coord. Chem. Rev.* **1998**, *177*, 347–414.
(33) Navarro, M.; Cisneros-Fajardo Efren, J.; Sierralta, A.; Fernandez-Mestre, M.; Silva, P.; Arrieche, D.; Marchan, E. *J. Biol. Inorg. Chem.* **2003**, *8*, 401–408.
(34) Delaney, S.; Pascaly, M.; Bhattacharya Pratip, K.; Han, K.; Barton, J. K. *Inorg. Chem.* **2002**, *41*, 1966–1974.
(35) Jia, C.; Liu, S.-X.; Tanner, C.; Leiggener, C.; Neels, A.; Sanguinet, L.; Levillain, E.; Leutwyler, S.; Hauser, A.; Decurtins, S. *Chem.—Eur. J.* **2007**, *13*, 3804–3812.
(36) Goze, C.; Leiggener, C.; Liu, S.-X.; Sanguinet, L.; Levillain, E.; Hauser, A.; Decurtins, S. *ChemPhysChem* **2007**, *8*, 1504–1512.
(37) Cardinaels, T.; Ramaekers, J.; Driesen, K.; Nockemann, P.; Van Hecke, K.; Van Meervelt, L.; Goderis, B.; Binnemans, K. *Inorg. Chem.* **2009**, *48*, 2490–2499.
(38) Gillard, R. D.; Hill, R. E. E.; Maskill, R. *J. Chem. Soc. A* **1970**, 1447–1451.
(39) Brusso, J. L.; Clements, O. P.; Haddon, R. C.; Itkis, M. E.; Leitch, A. A.; Oakley, R. T.; Reed, R. W.; Richardson, J. F. *J. Am. Chem. Soc.* **2004**, *126*, 8256–8265.
(40) Frei, M.; Diederich, F.; Tremont, R.; Rodriguez, T.; Echegoyen, L. *Helv. Chim. Acta* **2006**, *89*, 2040–2057.
(41) Kestemont, G.; de Halleux, V.; Lehmann, M.; Ivanov, D. A.; Watson, M.; Geerts, Y. H. *Chem. Commun.* **2001**, 2074–2075.
(42) Waterland, M. R.; Gordon, K. C.; McGarvey, J. J.; Jayaweera, P. M. *J. Chem. Soc., Dalton Trans.* **1998**, 609–616.

Dipyrido[3,2-*a*:2′,3′-*c*]phenazine-11,12 dithiol-15-thione (dppzS$_2$-CS) (2). Yield = 0.27 g, 87%. ^{1}H NMR (300 MHz CDCl$_3$) δ 9.60 (dd, 2H, J = 1.8 Hz, 8.4 Hz), 9.30 (dd, 2H, J = 4.5 Hz, 1.8 Hz), 8.45 (s, 2H), 7.83 (dd, 2H, J = 8.4 Hz, 4.5 Hz). Anal. Calcd for $C_{19}H_{12}N_4S_3 \cdot 2H_2O$ = C 53.75, H 2.85, N 13.20. Found: C 53.38, H 2.53, N 13.32. Mass spectrum was not available because of poor solubility.

Dipyrido[3,2-*a*:2′,3′-*c*]phenazine-11,12 bis (decaalkylthioether) (dppz(Sdec)$_2$). Yield = 0.213 g, 56% ^{1}H NMR (300 MHz CDCl$_3$) δ 9.58 (dd, 2H, J = 1.5 Hz, 8.1 Hz), 9.25 (dd, 2H, J = 1.5 Hz, 4.5 Hz), 7.99 (s, 2H), 7.77 (dd, 2H, J = 4.5 Hz, 8.1 Hz), 3.23 (t, 4H, J = 7.5 Hz), 1.89 (m, 4H), 1.58 (m, 4H), 1.28 (b, m, 24H), 0.88 (t, 6H, J = 6 Hz). Anal. Calcd for $C_{38}H_{50}N_4S_2$, C 72.70, H 8.04, N 8.94, S 10.23. Found: C 72.50, H 7.75, N 8.93, S 10.05. M/z (ESI POS): 627.3 {[dppz(Sdec)$_2$ + H$^+$}.

***fac*-Chlorotricarbonyl(dipyrido[3,2-*a*:2′,3′-*c*]phenazine-11,12 bis-(thiocyanate)-rhenium Re(dppz(SCN)$_2$)(CO)$_3$Cl.** Yield = 0.323 g, 92% ^{1}H NMR (300 MHz, CDCl$_3$) δ 9.82 (dd, 2H), 9.53 (dd, 2H), 8.97 (s, 2H), 8.10 (dd, 2H). Anal. Calcd for $C_{23}H_8N_6O_3S_2ReCl$, C 39.34, H 1.15, N 11.97. Found: C 39.40, H 1.29, N 11.90. (ESI POS): 666.9 {[Re(dppz(SCN)$_2$)(CO)$_3$]$^+$} ; 684.97 {[Re(dppz-(SCN)$_2$)(CO)$_3$]$^+$ + H$_2$O}.

***fac*-Chlorotricarbonyl(dipyrido[3,2-*a*:2′,3′-*c*]phenazine-11,12 dithiol-15-thione)-rhenium Re(dppzS$_2$CS)(CO)$_3$Cl.** Yield = 0.286 g, 80% ^{1}H NMR (300 MHz, CDCl$_3$) δ 9.79 (dd, 2H, J = 1.5, 8.4 Hz), 9.48 (dd, 2H, J = 1.5, 5.1 Hz), 8.52 (s, 2H), 8.04 (dd, 2H, J = 5.1, 8.4 Hz). Anal. Calcd for $C_{22}H_8N_4O_3S_3ReCl$, C 38.06, H 1.16, N 8.07, S 13.86. Found: C 37.81, H 1.27, N 7.99, S 13.81 M/z (ESI POS): 716.8 {[Re(dppzS$_2$CS)(CO)$_3$Cl] + Na+}.

***fac*-Chlorotricarbonyl(dipyrido[3,2-*a*:2′,3′-*c*]phenazine-11,12bis-(decaalkylthioether)-rhenium Re(dppz(Sdec)$_2$)(CO)$_3$Cl.** Yield = 0.28 g, 82% ^{1}H NMR (300 MHz, CDCl$_3$) δ 9.73 (dd, 2H, J = 1.5, 8.1 Hz), 9.42 (dd, 2H, J = 1.5, 5.1 Hz), 7.98 (s, 2H), 7.97 (m, 2H), 3.26 (t, 4H, J = 7.5 Hz), 1.925 (m, 4H), 1.60 (m, 4H), 1.28 (m, 24H), 0.88 (t, 6H, J = 7.2 Hz). Anal. Calcd for $C_{41}H_{50}N_4O_3S_2$-ReCl, C 52.8, H 5.4, N 6.01. Found: C 52.68, H 5.61, N 6.12. M/z (ESI POS): 955.5 {[Re(dppz(Sdec)$_2$)(CO)$_3$Cl] + Na$^+$}.

Physical Measurements. Aldrich spectroscopic grade or H.P. grade solvents were used for all spectroscopic measurements. Spectral data were analyzed by using GRAMS/32 AI (Galactic Industries) software. Mass spectrometry measurements were acquired from a Micromass LCT instrument for electrospray measurement or using a Shimadzu QP8000 alpha with ESI probe. Microanalyses were carried out at the Campbell Microanalysis Laboratory at the University of Otago.

Absorption spectra were measured at room temperature on a Varian Cary 500 Scan UV/vis/NIR spectrophotometer with Cary WinUV scan application software. A scan rate of 600 nm min^{-1} was employed between 200 and 800 nm. Samples were between 10^{-5} and 10^{-6} M in dichloromethane.

FT-Raman spectra were collected on powder samples using a Bruker IFS-55 interferometer with a FRA/106 S attachment. The excitation source was a Nd:YAG laser with an excitation wavelength of 1064 nm. A liquid nitrogen cooled Ge diode (D418T) was used to detect Raman photons. All spectra were measured over 64−256 scans with a laser power of 80 mW at the sample and spectral resolution of 4 cm^{-1}.

Resonance Raman spectra were recorded for all compounds by using a setup described previously.[43−46] Excitation wavelengths of 351, 407, 413, and 444 nm were employed and solutions were typically 5−7 mM in dichloromethane solution.

Table 1. Crystal Data for dppz(SCN)$_2$

	dppz(SCN)$_2$	
chemical formula	$C_{20}H_{18}N_6S_2$	
formula weight	396.44	
temperature	89(2) K	
wavelength	0.71073 Å	
crystal system	triclinic	
space group	$P\bar{1}$	
unit cell dimensions	a = 8.780 Å	α = 95.95°
	b = 9.792 Å	β = 112.13°
	c = 10.400 Å	γ = 95.38°
volume	815.2 Å^3	
Z	2	
density (calculated)	1.615 Mg/mm^3	
absorption coefficient	0.348 mm^{-1}	
F(000)	404	
crystal size	0.32 × 0.32 × 0.06 mm^3	
θ range for data collection	2.11−27.00	
index ranges	$-11 \le h \le 11$	
	$-12 \le k \le 12$	
	$-13 \le l \le 13$	
reflections collected	25533	
independent reflections	3570 [R(int) = 0.0245]	
completeness to θ = 27.00	99%	
absorption correction	semiempirical from equivalents	
max. and min transmisson	1.000000 and 0.884893	
refinement method	full-matrix least-squares on F^2	
data/restraints/parameters	3570/0/253	
goodnes -of-fit on F^2	1.012	
final R indices [$I > 2\sigma(I)$]	R1 = 0.0275, w R2 = 0.0801	
R indices (all data)	R1 = 0.0306, wR2 = 0.0829	
largest diff. peak and hole	0.475 and −0.288 e·Å^{-3}	

Single crystals of suitable quality for X-ray diffraction of dppz(SCN)$_2$ were grown from a concentrated chlorobenzene solution. Crystal data, data collection, and refinement parameters are listed in Table 1. Measurements were made with a Bruker diffractometer equipped with an Apex II charge-coupled device (CCD) area detector using graphite monochromated Mo Kα (λ = 0.71073 Å) radiation. The structure was solved by direct methods and refined on F^2 by use of all data in full-matrix least-squares procedures, with all non-hydrogen atoms refined anisotropically.

The electrochemical cell for cyclic voltammetry was made up of a 1 mm diameter platinum rod working electrode embedded in a KeL-F cylinder with a platinum auxiliary electrode and a Ag/AgCl reference electrode. The potential of the cell was controlled by an EG&G PAR 273 A potentiostat with model 270 software. Solutions were typically about 10^{-3} M in dichloromethane with 0.1 M tetrabutylammonium hexafluorophosphate (TBAPF$_6$) as supporting electrolyte, and were purged with nitrogen for approximately 5 min prior to measurement. The TBAPF$_6$ was recrystallized from ethyl acetate and dried under reduced pressure at 70 °C for 10 h, and then kept at 90 °C until use. The scanning speed was 1 V s^{-1}, and the cyclic voltammograms were calibrated against the decamethylferrocenium/decamethylferrocene (DMFc) couple (−0.012 V in CH$_2$Cl$_2$) and are reported relative to the saturated calomel electrode (SCE) for comparison with other data by subtracting 0.045 V.[47]

Computational Methods. Calculations were performed by using the Gaussian 03 package[48] and GaussSum 2.1.[49] In vacuo geometry optimizations and calculation of harmonic vibrational frequencies were performed by DFT, employing the B3LYP or CAM-B3LYP functional. Time-dependent density

(43) Howell, S. L.; Gordon, K. C. *J. Phys. Chem. A* **2004**, *108*, 2536–2544.
(44) Lind, S. J.; Gordon, K. C.; Waterland, M. R. *J. Raman Spectrosc.* **2008**, *39*, 1556–1567.
(45) Lind, S. J.; Walsh, T. J.; Blackman, A. G.; Polson, M. I. J.; Irwin, G. I. S.; Gordon, K. C. *J. Phys. Chem. A* **2009**, *113*, 3566–3575.
(46) Horvath, R.; Otter, C. A.; Gordon, K. C.; Brodie, A. M.; Ainscough, E. W. *Inorg. Chem.* **2010**, *49*, 4073–4083.
(47) Bard, A. J.; Faulkner, L. R., *Electrochemical Methods*, 2 ed.; John Wiley and Sons, Inc.: New York, 2001.

functional theory (TD-DFT) calculations were performed with a dichloromethane solvent field on the geometry obtained from the in vacuo calculation, as the in vacuo TD-DFT were unsatisfactory. Solvent calculations were implemented using the keyword *iefpcm* for dichloromethane. This implements a self-consistent reaction field method; the integral equation formalism polarizable continuum model, in which the solvent is considered as a continuum of a determined dielectric constant and the solute is within a cavity of the solvent and is modeled as a series of interlocked spheres.[50−52] If the excitation is charge-transfer in nature, TD-DFT using the B3LYP functional can underestimate the energy of charge-transfer transitions.[53] It has been suggested that the primary origin of this effect is self-interaction error.[54] The use of long-range corrected coulomb attenuated hybrids such as CAM-B3LYP have been shown to overcome this problem.[55] To test this in our systems TD-DFT calculations were performed using B3LYP and CAM-B3LYP functionals; we find that the CAM-B3LYP overestimated the transition energies (see Table S2, Supporting Information) for the ligands and complexes and thus we have used the B3LYP calculations in our interpretation of the data, as these calculations more closely predicted the experimental data.

The LANL2DZ core potential and associated basis set was used previously to describe the rhenium atom of analogous complexes.[56] Calculated frequencies were scaled by a factor of 0.975. Illustration of the vibrational modes was achieved using the Molden package.[57]

Results and Discussion

I. Modeling and Structure. The structures of the ligands and complexes were modeled using DFT (B3LYP) with a LANL2DZ basis set for rhenium and 6-31G(d) for the other atoms. In the absence of crystallographic data a comparison of modeled vibrational spectral data with experiment offers a good method of validating the calculations.[58−63] Our analyses of the Raman data sets reveals a mean absolute deviation of 7 cm^{-1} on bands of moderate to strong intensity; we consider this a good correlation (Figure 3).[64,65] Importantly this means that these calculations offer some insight into the electronic character of the ligands and how the electronic structure is altered by chelation to a metal.

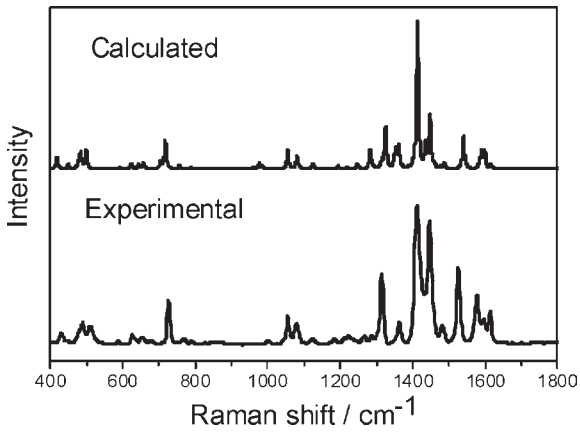

Figure 3. Comparison between the experimental and calculated FT-Raman spectra of $Re(dppz(Sdec)_2)(CO)_3Cl$.

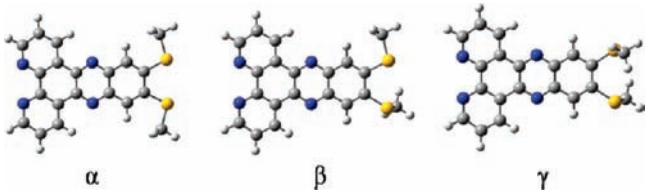

Figure 4. Structures of $dppz(Sdec)_2$ rotamers.

An analysis of the calculated structural data is unsurprising with one exception; the relative disposition of the $S\text{-}CH_3$ groups on the $dppz(Sdec)_2$ ligand (modeled as $dppz(SMe)_2$ to reduce computational expense) reveals that there are three rotamers of similar energy (Figure 4). Frequency calculations performed on each rotamer, showed there were no imaginary frequencies, indicating that each rotamer is a local minimum energy structure. The alpha rotamer has the lowest calculated energy difference relative to the beta and gamma rotamer structures and also the lowest mean absolute deviation (MAD) between calculated and experimental FT-Raman spectra. All calculated results presented for $dppz(Sdec)_2$ and $Re(dppz(Sdec)_2)(CO)_3Cl$ therefore pertain to the alpha rotamer.

It was possible to obtain a crystal structure of the $dppz(SCN)_2$ ligand; this crystallizes in the triclinic space group $P\bar{1}$. The dppz skeleton is virtually planar showing a mean deviation of 0.039 Å with a maximum deviation of

(48) Frisch, M. J.; Trucks, G. W.; Schlegel, H. B.; Scuseria, G. E.; Robb, M. A.; Cheeseman, J. R.; Montgomery, J. A., Jr.; Vreven, T.; Kudin, K. N.; Burant, J. C.; Millam, J. M.; Iyengar, S. S.; Tomasi, J.; Barone, V.; Mennucci, B.; Cossi, M.; Scalmani, G.; Rega, N.; Petersson, G. A.; Nakatsuji, H.; Hada, M.; Ehara, M.; Toyota, K.; Fukuda, R.; Hasegawa, J.; Ishida, M.; Nakajima, T.; Honda, Y.; Kitao, O.; Nakai, H.; Klene, M.; Li, X.; Knox, J. E.; Hratchian, H. P.; Cross, J. B.; Adamo, C.; Jaramillo, J.; Gomperts, R.; Stratmann, R. E.; Yazyev, O.; Austin, A. J.; Cammi, R.; Pomelli, C.; Ochterski, J. W.; Ayala, P. Y.; Morokuma, K.; Voth, G. A.; Salvador, P.; Dannenberg, J. J.; Zakrzewski, V. G.; Dapprich, S.; Daniels, A. D.; Strain, M. C.; Farkas, O.; Malick, D. K.; Rabuck, A. D.; Raghavachari, K.; Foresman, J. B.; Ortiz, J. V.; Cui, Q.; Baboul, A. G.; Clifford, S.; Cioslowski, J.; Stefanov, B. B.; Liu, G.; Liashenko, A.; Piskorz, P.; Komaromi, I.; Martin, R. L.; Fox, D. J.; Keith, T.; Al-Laham, M. A.; Peng, C. Y.; Nanayakkara, A.; Challacombe, M.; Gill, P. M. W.; Johnson, B.; Chen, W.; Wong, M. W.; Gonzalez, C.; Pople, J. A. *Gaussian 03*; Gaussian, Inc.: Pittsburgh, PA, 2003.
(49) O'Boyle, N. M.; Tenderholt, A. L.; Langner, K. M. *J. Comput. Chem.* **2008**, *29*, 839–845.
(50) Cances, E.; Mennucci, B.; Tomasi, J. *J. Chem. Phys.* **1997**, *107*, 3032–3041.
(51) Mennucci, B.; Tomasi, J. *J. Chem. Phys.* **1997**, *106*, 5151–5158.
(52) Cances, E.; Mennucci, B. *J. Chem. Phys.* **2001**, *115*, 6130–6135.
(53) Fink, R. F.; Pfister, J.; Zhao, H. M.; Engels, B. *Chem. Phys.* **2008**, *346*, 275–285.
(54) Dreuw, A.; Head-Gordon, M. *J. Am. Chem. Soc.* **2004**, *126*, 4007–4016.
(55) Kobayashi, R.; Amos, R. D. *Chem. Phys. Lett.* **2006**, *420*, 106–109.
(56) Dattelbaum, D. M.; Martin, R. L.; Schoonover, J. R.; Meyer, T. J. *J. Phys. Chem. A* **2004**, *108*, 3518–3526.
(57) Schaftenaar, G.; Noordik, J. H. *J. Comput. Aided Mol. Des.* **2000**, *14*, 123–134.
(58) Cleland, D. M.; Irwin, G.; Wagner, P.; Officer, D. L.; Gordon, K. C. *Chem.—Eur. J.* **2009**, *15*, 3682–3690.
(59) Lundin, N. J.; Blackman, A. G.; Gordon, K. C.; Officer, D. L. *Angew. Chem., Int. Ed.* **2006**, *45*, 2582–2584.
(60) Lundin, N. J.; Walsh, P. J.; Howell, S. L.; Blackman, A. G.; Gordon, K. C. *Chem.—Eur. J.* **2008**, *14*, 11573–11583.
(61) Karnahl, M.; Tschierlei, S.; Kuhnt, C.; Dietzek, B.; Schmitt, M.; Popp, J.; Schwalbe, M.; Krieck, S.; Goerls, H.; Heinemann, F. W.; Rau, S. *Dalton Trans.* **2010**, *39*(9), 2359–2370.
(62) Kuhnt, C.; Tschierlei, S.; Karnahl, M.; Rau, S.; Dietzek, B.; Schmitt, M.; Popp, J. *J. Raman Spectrosc.* **2010**, DOI: 10.1002/jrs.2534.
(63) Howell, S. L.; Gordon, K. C.; Waterland, M. R.; Leung, K. L.; Phillips, D. L. *J. Phys. Chem. A* **2006**, *110*, 11194–11199.
(64) Earles, J. C.; Gordon, K. C.; Officer, D. L.; Wagner, P. *J. Phys. Chem. A* **2007**, *111*, 7171–7180.
(65) Clarke, T. M.; Gordon, K. C.; Officer, D. L.; Hall, S. B.; Collis, G. E.; Burrell, A. K. *J. Phys. Chem. A* **2003**, *107*, 11505–11516.

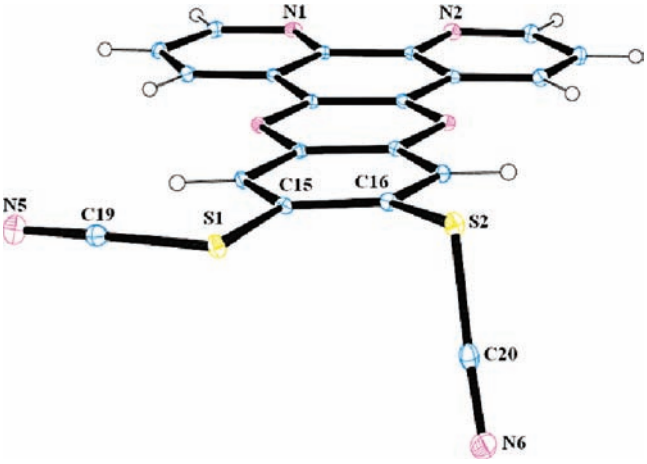

Figure 5. ORTEP diagram of dppz(SCN)$_2$ emphasizing the conformation of the SCN groups. Selected bond lengths (in angstroms): S(1)−C(19) 1.692(13); S1−C(15) 1.780(12); S(2)−C(20) 1.708(14); S(2)−C(16) 1.789-(12). Selected bond angles (in degrees): C(19)−S(1)−C(15) 100.44(6); C(20)−S(2)−C(16) 100.48(6).

Table 2. Carbonyl Stretching Frequencies (cm^{-1}) for Re(I)L(CO)$_3$Cl Complexes in CH_2Cl_2 Solution

compound	A′(1)	A″	A′(2)
Redppz(CO)$_3$Cl	2025	1923	1900
Re(dppz(SCN)$_2$)(CO)$_3$Cl	2026	1925	1903
Re(dppS$_2$CS)(CO)$_3$Cl	2025	1924	1901
Re(dppz(Sdec)$_2$)(CO)$_3$Cl	2025	1924	1901

0.072 Å for C16. A notable feature is the arrangement of the thiocyanate groups relative to the dppz skeleton (Figure 5). The torsion angle for the S2 SCN group out of the E-ring plane is 85.54° (calculated 83.3°) while the S1 SCN group is close to coplanar with the dppz framework (torsion angle = 1.98°, calculated 1.08°). Experimental and calculated bond lengths are in good agreement, with the C15−S1 bond length being the only one with greater than 0.02 Å difference between experimental and calculated values.

Vibrational Spectroscopy. The IR carbonyl stretching frequencies for the Re(L)(CO)$_3$Cl complexes in this study are presented in Table 2. The stretching frequency of the carbonyl group reports on the electron density at the metal center.[66,67] As can be seen, the frequencies for the three substituted dppz complexes and the parent dppz complex are very similar, indicating the different electronic effects of the sulfur-containing substituents do not affect the metal center. This is consistent with the segregated orbital model with disconnected phen and phz MOs.[2,11,20]

FT-Raman Spectroscopy. A table of selected FT-Raman bands, their calculated frequency, vibrational mode, and assignment is presented in the Supporting Information. A common feature for all compounds in this study is the strong band around 1400 cm^{-1} assigned as a phz vibration. A band at around 1320 cm^{-1} assigned as a phen-based vibration is present in all compounds except the dppzS$_2$CS ligand. Unique to dppzS$_2$CS and its Re(I) complex is a strong band at 1096 cm^{-1}, a C=S stretching mode of the trithiocarbonate adduct.

Table 3. ^{1}H NMR Data for Ligands and Re(I) Complexes

	phen			phz
compound	H 3, 6[a]	H 2,7	H 1,8	H 13,10
dppz(SCN)$_2$	9.34[b]	7.86	9.61	8.87
dppzS$_2$CS	9.30	7.83	9.60	8.45
dppz(Sdec)$_2$	9.25	7.77	9.58	7.99
dppz[c]	9.28	7.80	9.65	8.36
Re(dppz)(CO)$_3$Cl[c]	9.47(0.19)[d]	8.02(0.22)	9.87(0.22)	8.45(0.10)
Re(dppz(SCN)$_2$)(CO)$_3$Cl	9.53(0.19)	8.1(0.24)	9.82(0.21)	8.97(0.10)
Re(dppzS$_2$CS)(CO)$_3$Cl	9.48(0.18)	8.04(0.21)	9.79(0.19)	8.52(0.07)
Re(dppz(Sdec)$_2$)(CO)$_3$Cl	9.42(0.17)	7.97(0.14)	9.73(0.15)	7.98(0.01)

[a] Atom labeling shown in Figure 1. [b] Chemical shifts for all compounds referenced to $CDCl_3$ solvent peak at 7.260 ppm. [c] Chemical shifts for dppz and Re(dppz)(CO)$_3$Cl.[42] [d] Coordination induced shift (CIS) = $\delta_{(complex)} - \delta_{(ligand)}$ (shown in parentheses).

II. Physical Properties. The ^{1}H chemical shifts for substituted dppz ligands and their complexes give information regarding the electronic effects of the substituents on the ligand.[68] The singlet corresponding to H-13/10 is sensitive to the relative electron withdrawing/donating effects of the substituents at the 11 and 12 positions. Table 3 gives the ^{1}H NMR data for the dppz protons, for the ligands in this study as well as dppz itself. These data indicate that the electron withdrawing effects of the substituents can be ordered: thiocyanate > trithiocarbonate > thioether. The thioether substituents increase the electron density on the phenazine portion of the ligand. The chemical shifts for protons at the phen end of the ligand are relatively unaffected by substituents; this supports the view of segregated phen and phz MO model of dppz.[21]

The coordination induced shift (CIS) = $\delta_{(complex)} - \delta_{(ligand)}$ measures the difference in chemical shift of a signal between the coordinated and free ligand (Table 3). CIS parameters have been shown useful in probing the π back-bonding nature of metal polypyridyls.[69] The general trend is a small increase in chemical shift upon coordination of the ligands to Re(I). This increase is larger for the phen protons, that is, the protons closest to the Re(I) center. This deshielding upon coordination is expected to occur for two reasons: a reduction in electron density on the ligand resulting in a downfield shift, because of donation of σ electron density to form the two metal−ligand bonds, and the back-donation of π electron density from the Re(I) center to the ligand. These shifts of approximately 0.2 and 0.1 ppm for the phen and phz based protons, respectively, are similar to those of Re(dppz)(CO)$_3$Cl and other Re(I) complexes of substituted dppz complexes.[68]

Electrochemical Studies. Electrochemical data for the ligands and Re(I) complexes in dichloromethane are presented in Table 4. Many studies, both electrochemical and computational,[1,2,13,19,21] have shown that the lowest unoccupied molecular orbital (LUMO) of a wide range of dppzs ligands and their Re(I) complexes is phenazine-based. This conclusion is due to the reduction potential of dppz (−1.28 V vs SCE)[42] being much closer

(66) Alsindi, W. Z.; Easun, T. L.; Sun, X. Z.; Ronayne, K. L.; Towrie, M.; Herrera, J.; George, M. W.; Ward, M. D. *Inorg. Chem.* **2007**, *46*, 3696–3704.
(67) Grills, D. C.; Turner, J. J.; George, M. W. *Compr. Coord. Chem. II* **2004**, *2*, 91–101.
(68) Arancibia, A.; Concepcion, J.; Daire, N.; Leiva, G.; Leiva, A. M.; Loeb, B.; Del Rio, R.; Diaz, R.; Francois, A.; Saldivia, M. *J. Coord. Chem.* **2001**, *54*, 323–336.
(69) Garces, F. O.; Watts, R. J. *Magn. Reson. Chem.* **1993**, *31*, 529–536.

Table 4. Electrochemical Data for Ligands and Complexes

compound	E_{red}[a]/V vs SCE	ΔR[b]
dppz(SCN)$_2$	−0.85	
dppzS$_2$CS	−0.98	
dppz(Sdec)$_2$	−1.23	
dppz[c]	−1.28	
dppzCN[c]	−0.91	
dppzMe[c]	−1.30	
dppzoxad[c]	−0.85	
Re(dppz(SCN)$_2$)(CO)$_3$Cl	−0.63	0.22
Re(dppzS$_2$CS)(CO)$_3$Cl	−0.75	0.23
Re(dppz(Sdec)$_2$)(CO)$_3$Cl	−1.03	0.21
Re(dppz)(CO)$_3$Cl [c]	−1.01	0.27
Re(dppzCN)(CO)$_3$Cl [c]	−0.63	0.28
Re(dppzMe)(CO)$_3$Cl[c]	−1.04	0.26
Re(dppzoxad)(CO)$_3$Cl [c]	−0.75	0.1

[a] Reduction potentials are recorded against $DMFc^+$/DMFc and converted to SCE. Solvent CH_2Cl_2, supporting electrolyte $TBAPF_6$. Irreversible oxidations were observed toward the solvent limit. [b] The decrease in reduction potential upon coordination. [c] Previously studied, included for comparison.[60]

to that of phenazine (−1.4 V) than that of 2,2-bipyridine (−2.35 V).[1] The change in reduction potential is therefore a good indicator of alteration of the phz MO energy level by the substituent. The order of the ligand reduction potentials reflects the electron-withdrawing ability of the substituent as established from ^{1}H NMR, that is, the reduction potential of dppz(SCN)$_2$ > dppzS$_2$CS > dppz(Sdec)$_2$. This trend is again reflected in the Re(I) complexes, with an average decrease of 220 mV upon coordination, comparable to other Re(I) dppz complexes.[18,42,60]

Electronic Absorption Spectra−Time Dependent DFT Calculations. To understand the visible spectra of these ligands and their complexes it is instructive to relate the observed bands to (1) the TD-DFT results and (2) the resonance Raman band enhancements. TD-DFT has been successfully applied to the prediction of metal polypyridyl electronic transitions.[26,61,62,70−73]

It is generally found that the shifts in energies are well predicted, but the absolute values are offset; this is true for charge-transfer transitions as discussed by Dreuw and Head-Gordon.[54] The calculated and experimental data reflect the nature of the electronic transition of interest. The electronic absorption spectra of the ligands and their complexes are presented in Figures 6 and 7 respectively.

These spectra differ considerably from unsubstituted dppz and its Re(I) complex. The most striking difference is that for dppzS$_2$CS and dppz(Sdec)$_2$ the ligand spectra have strong absorption bands at 427 and 434 nm, significantly red-shifted from that of dppz (378 nm). Upon complexation this band is further red-shifted to 439 and 447 nm for Re(dppzS$_2$CS)(CO)$_3$Cl and Re(dppz(Sdec)$_2$)(CO)$_3$Cl, respectively.

The second difference occurs in the spectra of the Re complexes; for Re(dppzS$_2$CS)(CO)$_3$Cl and Re(dppz(Sdec)$_2$)(CO)$_3$Cl a band appears at around 330 nm which

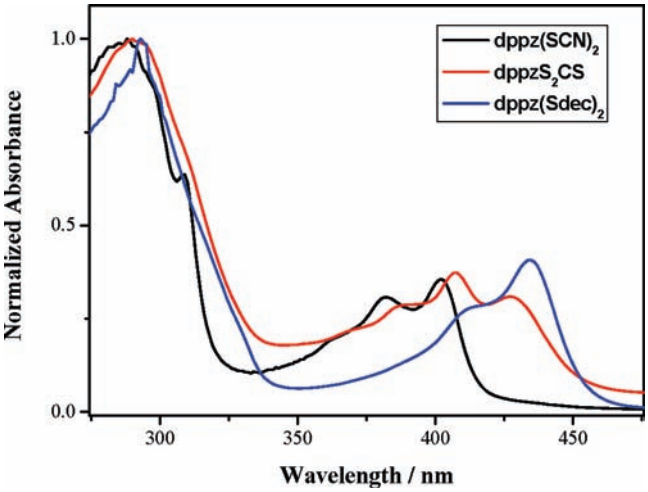

Figure 6. Electronic absorption spectra of the ligands recorded in CH_2Cl_2.

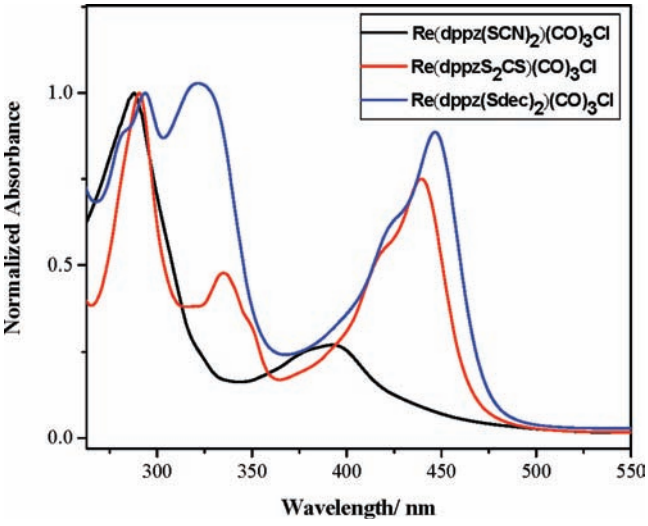

Figure 7. Electronic absorption spectra of the Re(I)L(CO)$_3$Cl complexes recorded in CH_2Cl_2.

is absent in the spectrum of Redppz(CO)$_3$Cl. Analyses of the TDDFT calculations show qualitative agreement with experimental absorption data. (Table 5)

The dppzS$_2$CS and dppz(Sdec)$_2$ ligands show bands that are significantly red-shifted from dppz and dppz(SCN)$_2$. For example dppzS$_2$CS and dppz(Sdec)$_2$ have lowest energy transitions predicted to lie at 401 and 404 nm respectively, whereas the lowest energy transitions for dppz and dppz(SCN)$_2$ are at 345 and 368 nm respectively (Table 5)

For the Re complexes the predicted UV visible data may be split into two groups; for Re(dppz)(CO)$_3$Cl and Re(dppz(SCN)$_2$)(CO)$_3$Cl, weak bands are predicted at 433 and 492 nm respectively (see Table 5), while for Re(dppzS$_2$CS)(CO)$_3$Cl and Re(dppz(Sdec)$_2$)(CO)$_3$Cl a very strong band is predicted at 410 and 434 nm respectively, similar to the transition observed in the corresponding ligands. The makeup of the LUMOs for dppzS$_2$CS and its Re(I) complex differ from those of dppz, dppz(SCN)$_2$ and dppz(Sdec)$_2$. There are a number of UMOs of dppz that lie close in energy; these have phz character (labeled 5b$_1$), phen character (4b$_1$), or are

(70) Gabrielsson, A.; Matousek, P.; Towrie, M.; Hartl, F.; Zalis, S.; Vlcek, A., Jr. *J. Phys. Chem. A* **2005**, *109*, 6147–6153.
(71) Turki, M.; Daniel, C.; Zalis, S.; Vlcek, A., Jr.; van Slageren, J.; Stufkens, D. J. *J. Am. Chem. Soc.* **2001**, *123*, 11431–11440.
(72) Vlcek, A.; Zalis, S. *Coord. Chem. Rev.* **2007**, *251*, 258–287.
(73) Rau, S.; Schwalbe, M.; Losse, S.; Goerls, H.; McAlister, C.; MacDonnell, F. M.; Vos, J. G. *Eur. J. Inorg. Chem.* **2008**, *7*, 1031–1034.

Table 5. Experimental and Calculated[a] Electronic Data for Complexes and Ligands

	λ/ nm[b]	ε[c]	λ/ nm[d]	f[e]	MO configurations, major components (% contribution)	changes in wave function amplitude with transition for the optical electron: sulfur adduct	phz	phen	metal
dppz	*379*	*12900*	345	0.29	H-1, L (79%)		59→71 (12)	41→29 (−12)	
	367	*11300*							
	270	*43700*	286	0.56	H, L+1 (16%); H-1, L+2 (−37%)		56→30 (−26)	44→70 (26)	
$dppz(SCN)_2$	*401*	*19700*							
	381	*17200*	368	0.36	H-1, L (85%)	9→3 (−6)	37→76 (39)	54→21 (−33)	
	287	*52400*	296	1.08	H, L+1 (62%)	22→4 (−18)	33→60 (27)	45→35 (−10)	
$dppzS_2CS$	*427*	*11100*							
	407	*13400*	401	0.88	H, L (85%)	47→18 (−29)	37→64 (27)	16→18 (2)	
	386	*10200*							
	290	*35900*	284	0.81	H-1, L+2 (35%); H, L+3 (−39%)	31→5 (−26)	39→29 (−10)	30→67 (37)	
$dppz(Sdec)_2$	*434*	*20350*	404	0.54	H, L (85%)	43→4 (−39)	44→72 (28)	14→24 (10)	
	409	*13500*							
	293	*49900*	305	0.62	H-1, L+1 (54%); H, L+2 (28%)	36→2 (−34)	45→36 (−9)	19→62 (43)	
			292	0.42	H-5, L (74%); H-1, L+1 (12%)	26→3 (−23)	28→68 (40)	46→28 (−18)	
$Re(dppz)(CO)_3Cl$			433	0.06	H-1, L (91%)		1→64 (63)	5→35 (30)	93→1 (−92)
	360	*13800*	340	0.18	H-4, L (71%); H-3, L+2 (24%)		68→60 (−8)	26→40 (14)	6→0 (−6)
	280	*50000*	289	0.83	H-7, L (−35%); H-3, L+2 (38%)		44→49 (5)	17→50 (33)	40→1 (−39)
			492	0.03	H-1, L (56%)	0→3 (3)	1→74 (73)	5→23 (18)	94→0 (−94)
$Re(dppz(SCN)_2)(CO)_3Cl$	*415*	*sh*	411	0.10	H-1, L+1 (89%)	0→0 (0)	1→6 (5)	5→87 (82)	94→7 (−87)
	393	*11200*	388	0.10	H-3, L (−22%); H, L+2 (72%)	6→3 (−3)	12→52 (40)	7→45 (38)	75→0 (−75)
	288	*41500*	299	0.55	H-4, L+1 (33%); H-3, L+2 (29%)	24→2 (−22)	36→36 (0)	31→59 (28)	9→3 (−6)
$Re(dppzS_2CS)(CO)_3Cl$	***439***	***53200***	**410**	**0.73**	**H-2,L (56%); H-1, L+1 (−35%)**[f]	**38→8 (−30)**	**19→41 (22)**	**6→48 (42)**	**38→3 (−35)**
	417	*sh*							
	335	**34000**	**317**	**0.80**	**H-4, L+2 (31%); H-2,L+3 (53%)**[g]	**44→54 (10)**	**39→20 (−19)**	**10→25 (15)**	**7→0 (−7)**
	291	*70800*							
$Re(dppz(Sdec)_2)(CO)_3Cl$	***447***	***49200***	**434**	**0.30**	**H-1, L (83%)**[f]	**23→4 (−19)**	**21→62 (41)**	**9→34 (25)**	**47→1 (−46)**
	424	*sh*	410	0.26	H-2, L (81%)	28→4 (−24)	22→63 (41)	4→33 (29)	46→0 (−46)
	321	***55600***	**331**	**0.86**	**H-3, L+2 (86%)**[g]	**40→1 (−39)**	**50→33 (−17)**	**8→65 (57)**	**1→1 (0)**
	294	*51500*							

[a] Calculations were run with a solvent field, see Experimental Section. [b] Experimental absorption maxima. [c] Experimental extinction coefficient ($L\,mol^{-1}\,cm^{-1}$). [d] Calculated absorption maxima. [e] Calculated oscillator strength. [f] Transition may be best described as sulfur to dppz and metal to dppz, see Figure 8 and text for details. [g] Transition may be best described as sulfur to dppz, see Figure 8 and text for details.

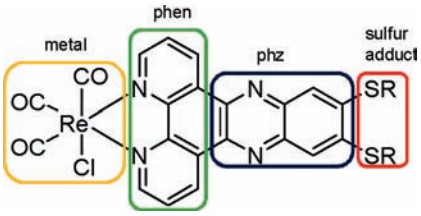

Figure 8. Re(I) dppz molecule sectioned into portions for calculated transition charge changes.

delocalized ($4a_2$). In addition to these UMOs, $dppzS_2CS$ possesses a LUMO+1 (Figure 9) which is a non bonding orbital with 80% of its character on the trithiocarbonate adduct. This orbital becomes LUMO+3 in the complex with 85% density on the S moiety, as the phen and delocalized MOs are stabilized in energy, becoming LUMO+1 and LUMO+2 respectively.

The transitions that are predicted may be classified based on orbital percentage, and specifically, the role of the S atoms in the transitions. The level of charge transfer that involves the S atoms for ligands and complexes may be parametrized by integrating electronic charge changes with transition as a function of sections of the molecule. This is

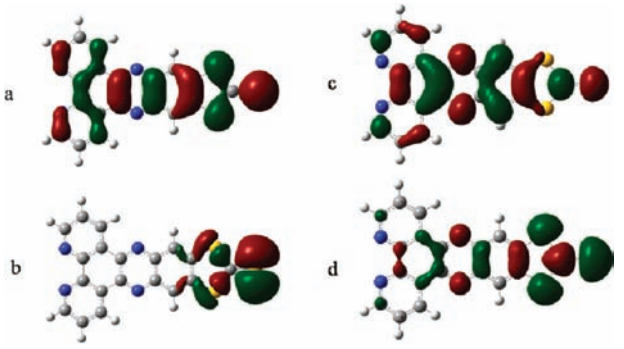

Figure 9. Selelcted MOs of $dppzS_2CS$: a, HOMO; b, HOMO-2; c, LUMO ($4b_2$) ; d, LUMO+1.

achieved with a Mulliken charge partitioning scheme which describes charge distribution throughout a molecule by assigning partial charges to atoms.[74] The partitioning of the atoms into the domains, phen, phz, S adduct, and metal (for the complexes) is depicted in Figure 8.

(74) Zalis, S.; Farrell, I. R.; Vlcek, A., Jr. *J. Am. Chem. Soc.* **2003**, *125*, 4580–4592.

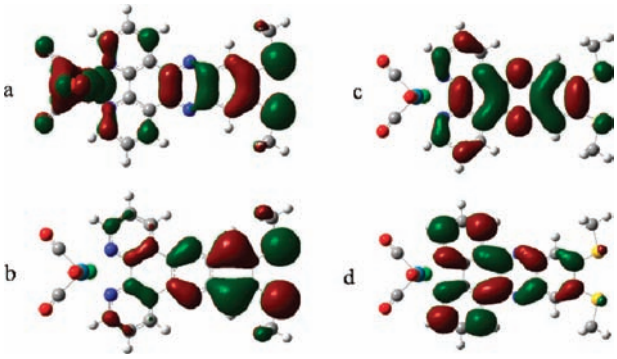

Figure 10. Selected MOs of Re(dppz(Sdec)$_2$)(CO)$_3$Cl: a, HOMO-1; b HOMO-3; c, LUMO; d, LUMO+2 (4a$_2$). Additional MOs of the ligands and complexes are shown in Tables S3 and S4 (Supporting Information).

The level of electron density changes associated with particular transitions is shown in Table 5. For these data the strong transition observed in dppz(Sdec)$_2$ and dppzS$_2$CS is dominated by a S → phz transition, which differs from the lowest lying transition of dppz and dppz(SCN)$_2$ which is a $\pi \rightarrow \pi^*$ transition of the dppz framework. In the case of dppz(SCN)$_2$ there is some S character in this transition, but it is very small compared to that for the dppzS$_2$CS and dppz(Sdec)$_2$ transitions. For all of the ligands a second higher energy transition is present; this is best described as a delocalized LC $\pi \rightarrow \pi^*$ transition in which donor and acceptor MOs are both delocalized and are not polarized toward the S atoms. For the metal complexes there are some differences in the predicted UV−vis spectra. First an MLCT transition is predicted for Re(dppz)(CO)$_3$Cl which is dominated by a dπ→phen transition. This transition shifts to the red for Re(dppz(SCN)$_2$)(CO)$_3$Cl and consistent with this shift the predicted MOs associated with the transition are more delocalized, comprising dπ→phen and dπ→phz transitions. In the case of Re(dppz(Sdec)$_2$)(CO)$_3$Cl, the strong absorption at 447 nm (predicted at 434 nm) is also attributed to an ICT. The calculated donor MOs for this transition (HOMO-1 and HOMO-2) retain their sulfur character from the free ligand, but also contain significant density on the metal center (Figure 10). One can therefore think of this as a charge transfer transition from both the metal and the sulfur portions to the phenazine LUMO. For Re(dppzS$_2$CS)(CO)$_3$Cl the electronic transitions that comprise the strong absorption at 439 nm (predicted 410 nm) are dπ→phen and S → phz with the ICT being the dominant configuration. The net charge transfer is similar to that of Re(dppz(Sdec)$_2$)(CO)$_3$Cl, that is, charge transfer from the metal and sulfur adduct to the accepting phz MO. With this in mind it is interesting to note there is a negligible solvatochromic effect for the Re(dppzS$_2$CS)(CO)$_3$Cl and Re(dppz(Sdec)$_2$)(CO)$_3$Cl complexes.

The higher energy transition observed in Re(dppzS$_2$CS)(CO)$_3$Cl at 335 nm and in Re(dppz(Sdec)$_2$)(CO)$_3$Cl at 321 nm is accounted for in the calculations. The greater intensity of this transition in Re(dppz(Sdec)$_2$)(CO)$_3$Cl (5.56×10^4 L mol^{-1} cm^{-1}) over Re(dppzS$_2$CS)(CO)$_3$Cl (3.4×10^4 L mol^{-1} cm^{-1}) may be explained by the parent molecular orbitals and the subsequent charge distribution. The transition responsible in Re(dppz(Sdec)$_2$)(CO)$_3$Cl is HOMO-3 → LUMO+2. The donor orbital is a delocalized ligand orbital with high density on the sulfur (41%) and phz (51%) portions. The acceptor LUMO+2 orbital (4a$_2$ delocalized) has its density on the phen (66%) and phz (32%) regions, the net result being an increase in charge on the phen portion of the dppz, thus indicating a pseudocharge transfer from the sulfur to the phen, although involving two delocalized MOs. The corresponding transition in Re(dppzS$_2$CS)(CO)$_3$Cl involves HOMO-4 → LUMO+2 and HOMO-2 → LUMO+3, the latter being the dominant contribution. On inspection the HOMO-4 → LUMO+2 transition would result in a similar S → phen pseudo CT transition as in Re(dppz(Sdec)$_2$)(CO)$_3$Cl. However, the dominant acceptor MO LUMO+3, the MO unique to Re(dppzS$_2$CS)(CO)$_3$Cl having 85% of its electron density on the S$_2$CS adduct, counteracts any 'S → phen' behavior of the HOMO-4 → LUMO+2. The sum charge transfer of these transitions is therefore much more diffuse than that of Re(dppz(Sdec)$_2$)(CO)$_3$Cl (S$_2$CS 10, Phz −19, Phen 15, Metal −7) perhaps explaining the lower intensity of the 320 nm transition in Re(dppzS$_2$CS)(CO)$_3$Cl.

It is interesting to note that the HOMO does not play as significant a role in the configurations that make up many of the transitions for the metal complexes. The HOMO has χ symmetry with respect to the ligand N atoms;[75] however the LUMO and LUMO+1 which dominate the configurations of the lower energy transitions are of ψ symmetry. Thus HOMO, LUMO and HOMO, LUMO+1 interactions are symmetry disallowed.

Resonance Raman spectroscopy. In addition to the theoretical studies it is possible to probe the nature of the observed electronic transitions using resonance Raman spectroscopy.[76] The resonance Raman effect produces strong Raman band intensity enhancements as a consequence of the vibronic coupling of normal coordinates with electronic transitions.[77] The observed enhancements of intensity is not random across the normal modes of the probed molecule; rather those modes that mimic the nature of the electronic photoexcitation show preferential enhancement.[78] Hence vibrational modes that are enhanced are associated with the structural distortions attendant upon the active chromophore. A number of studies have examined the Raman spectra of dppz-type ligands and their complexes in concert with DFT calculations.[61,62,73] Examination of the resonance Raman spectra of Re(dppz(SCN)$_2$)(CO)$_3$Cl shows that the major bands present in the normal Raman spectrum, that is, those at 1400 and 1447 cm^{-1} remain strong features as the excitation wavelength is tuned across the main visible absorption band. This is consistent with the TDDFT data which predicts the main lowest lying absorption feature of Re(dppz(SCN)$_2$)(CO)$_3$Cl to be a composite of dπ→phen and dπ→phz MLCT transitions. Such transitions would enhance the modes associated with 1400 and 1447 cm^{-1} and these are phz stretch and delocalized modes respectively. For Re(dppz(Sdec)$_2$)(CO)$_3$Cl using the excitation wavelengths 407, 413, and 444 nm, a distinct enhancement of the bands at 1221 and

(75) Orgel, L. E. *J. Chem. Soc.* **1961**, 3683–3686.
(76) Horvath, R.; Gordon, K. C. *Coord. Chem. Rev.* **2009**, DOI: 10.1016/j.ccr.2009.11.015.
(77) Clark, R. J. H.; Dines, T. J. *Angew. Chem.* **1986**, *98*, 131–160.
(78) Hirakawa, A. Y.; Tsuboi, M. *Science* **1975**, *188*, 359–361.

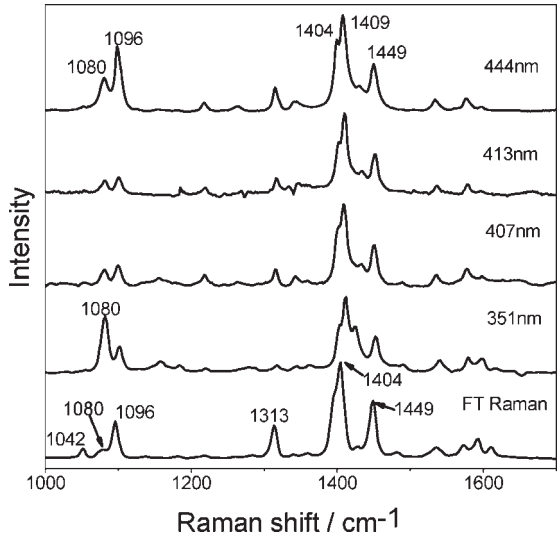

Figure 11. Resonance Raman spectra of Re(dppzS$_2$CS)(CO)$_3$Cl generated with different excitation wavelengths. FT-Raman spectrum was measured on a powder sample; all other spectra were obtained from 5 mM CH_2Cl_2 solutions.

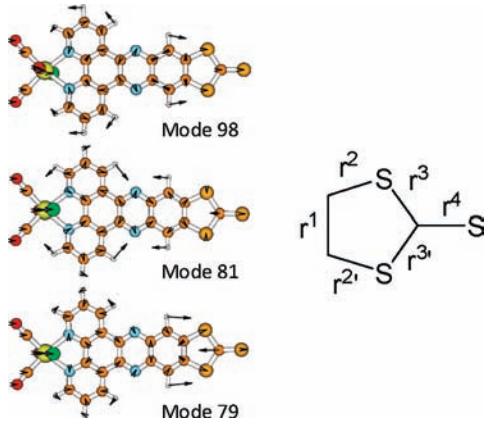

Figure 12. Eigenvector diagrams for selected vibrational modes showing displacement vectors of Re(dppzS$_2$CS)(CO)$_3$Cl. The bond designations r_1 through r_5 for the trithiocarbonate adduct are also shown.

1427 cm^{-1} relative to the FT Raman data is observed, and there is a diminution of the 1314 cm^{-1} band. The enhanced band at 1221 cm^{-1} (mode 93) is assigned to a phz vibration. The 1427 cm^{-1} band is a phz vibration, but also with significant E ring character (Supporting Information,Table S1). The enhancement of these modes is consistent with the S → phz assignment of the transition. The diminution of the 1314 cm^{-1} band, assigned as a phen mode, supports this. The 351 nm resonance Raman shows a different set of features including the enhancement of the 1578 cm^{-1} band (mode 118). This band is assigned as a delocalized vibration, in which there is also significant E ring bond distortion. This is consistent with the assignment from the TD-DFT data (Table 5) in which this band is attributed to a delocalized transition.

The resonance Raman spectrum of Re(dppzS$_2$CS)(CO)$_3$Cl (Figure 11) generated with 444 nm excitation shows enhancement of the 1096 cm^{-1} (mode 81) C=S based mode, and the 1409 and 1449 cm^{-1} phz vibrations. This is consistent with an S → phz assignment. The resonance Raman spectrum generated with 351 nm excitation shows the enhancement of the 1080 cm^{-1} band (mode 79) which is also a C=S based vibration.

This is a different mode than the one enhanced in the 444 nm spectra, indicating a different orbital parentage between the transitions probed, even though both transitions involve the S$_2$CS substituent. An examination of the two resonantly enhanced S$_2$CS modes shows that they distort the S$_2$CS group in slightly different ways. The band enhancement with 351 nm excitation (mode 79) (Figure 12) may be described as $r_4 + r_2 + r_2'$; the band enhanced with 444 nm excitation (mode 81) has $r_4 - r_2 - r_2'$ character. The enhancement of mode 81 is consistent with the TD-DFT data in that the electronic transition attributed to this excitation has a donor MO (HOMO-2) with antibonding r_2,r_2' character populating an acceptor MO with antibonding r_4 character but non bonding across r_2 and r_2'. Thus this will distort the S$_2$CS along r_2 and r_2' as a compression or shortening of bond length and elongate the r_4 bond. For the 351 nm excitation a different orbital parentage is active; the donor MO is antibonding along r_2, r_2' (HOMO −2), but in this case the acceptor MO (LUMO+3) is antibonding along r_4 r_2 r_2'. Thus elongation of all three bonds will accompany photoexcitation at this wavelength. Also enhanced at 351 nm is the 1424 cm^{-1} band (mode 98), assigned as a delocalized vibration, with a large perturbation of the E ring.

Common among the Re(dppzS$_2$CS)(CO)$_3$Cl and Re(dppz(Sdec)$_2$)(CO)$_3$Cl complexes is the enhancement of bands involving significant E ring/sulfur bond perturbation, confirming the orbital parentage responsible as the sulfur based MOs. Absent, however, from this analysis are the carbonyl stretching modes that would be commonly found in the resonance Raman spectra of MLCT transitions. If the low energy transitions of Re(dppzS$_2$CS)(CO)$_3$Cl and Re(dppz(Sdec)$_2$)(CO)$_3$Cl are in fact ICT transitions involving the metal center, one might expect enhancement of these carbonyl bands across the red wavelengths (407−444 nm). The calculated TD-DFT data suggest that these transitions, normally assigned as MLCT in nature because of their low energy, are not dominated by dπ to π^* configurations but also involve other electronic configurations which reduce the effective MLCT. Therefore the enhancement of the carbonyl bands is not as strong in these compounds compared to Redppz(CO)$_3$Cl where such additional configurations do not contribute to the low energy transitions.[76]

Conclusions

The synthesis and characterization of a series of sulfur-substituted dppz ligands and their Re(I) complexes are reported. The sulfur substituents reveal some interesting electronic properties that are atypical of dppz ligands and their complexes. In the case of the dppz(SCN)$_2$ the properties of both the ligand and Re(I) complex are similar to those observed for other dppz systems with electron-withdrawing substituents on the phenazine. For dppzS$_2$CS and dppz(Sdec)$_2$ the substituents are strongly electron donating leading to some atypical and unique properties for the ligands and the respective Re(I) complexes. First the infrared data of the complexes reveals that the S-substituents have only a minor effect on the backbonding of the Re. NMR studies reveal that the electron density about the phz ring is strongly perturbed by the substituents, with the SCN substituent reducing the

electron density at the phz, the S_2CS being similar to the dppz, and the Sdec being electron donating; the Sdec also shows the smallest shift in the phz ^1H signals on coordination to $Re(I)(CO)_3Cl$. The electrochemistry reveals that all of the S-substituted dppz ligands are easier to reduce than dppz, with the electron withdrawing $dppz(SCN)_2$ being the easiest; however, on coordination all three Re(I) complexes show a slightly smaller stabilization to reduction relative to dppz (200 versus 270 mV). The electronic absorption spectra of the ligands $dppz(Sdec)_2$ and $dppzS_2CS$ show the presence of a low energy band attributed to a S → phz ICT transition. Furthermore, the Re(I) complexes of these ligands show some shifts of this low energy transition, and calculations reveal that the nature of the transition is a mixture of MLCT and S → phz; the system is effectively donating electrons to the phz from two different directions. This interpretation is supported by the resonance Raman data that show enhancements of vibrations attributable to the sulfur substituents. The partial oxidation of the metal center in the mixed excited state results in the absence of the usual carbonyl band enhancement observed in the resonance Raman spectra of $Re(I)(CO)_3Cl$ polypyridyl MLCT transitions.

Both $Re(dppzS_2CS)(CO)_3Cl$ and $Re(dppz(Sdec)_2)(CO)_3Cl$ possess a higher energy transition around 330 nm atypical of $Re(dppz)(CO)_3Cl$ type complexes. This transition is assigned as pseudo S → phen ICT and is more intense in $Re(dppzSdec)_2)(CO)_3Cl$ than $Re(dppzS_2CS)(CO)_3Cl$. Examination of the orbitals from TD-DFT calculations show a unique UMO (LUMO+3) on $Re(dppzS_2CS)(CO)_3Cl$ which has high density on the S_2CS adduct, thus resulting in a more diffuse transition with lower intensity compared to that of $Re(dppzSdec)_2)(CO)_3Cl$. Resonance Raman excitation of $Re(dppzS_2CS)(CO)_3Cl$ at 351 and 444 nm results in enhancement of different vibrational modes; this pattern of enhancements of the S_2CS moiety may be rationalized with respect to the orbitals attributed to the transitions through calculations.

Acknowledgment. We thank the University of Otago, the Royal Society of New Zealand (Marsden Fund UOO611), the MacDiarmid Institute for Advanced Materials and Nanotechnology, and the Foundation of Research Science and Technology for support for this project.

Supporting Information Available: X-ray crystallographic data of $dppz(SCN)_2$ ligand in CIF format. FT-Raman data for complexes and ligands (Table S1). TD-DFT data from CAM-B3LYP calculations (Table S2). Frontier MO diagrams for ligands and complexes (Tables S3 and S4 respectively). This material is available free of charge via the Internet at http://pubs.acs.org.